Bound States in the Continuum in Open Aharonov–Bohm Rings¶

E. N. Bulgakov[a], K. N. Pichugin[a], A. F. Sadreev[a], and I. Rotter[b]

[a] Institute of Physics, Russian Academy of Sciences, Krasnoyarsk, 660036 Russia
[b] Max-Planck-Institut für Physik komplexer Systeme, D-01187 Dresden, Germany

Received September 4, 2006

Using the formalism of the effective Hamiltonian, we consider bound states in a continuum (BIC). They are nonhermitian effective Hamiltonian eigenstates that have real eigenvalues. It is shown that BICs are orthogonal to open channels of the leads, i.e., disconnected from the continuum. As a result, BICs can be superposed to a transport solution with an arbitrary coefficient and exist in a propagation band. The one-dimensional Aharonov–Bohm rings that are opened by attaching single-channel leads to them allow exact consideration of BICs. BICs occur at discrete values of the energy and magnetic flux; however, it's realization strongly depends on the way to the BIC point.

1. INTRODUCTION

In 1929, von Neumann and Wigner [1] first pointed to the existence of discrete solutions of the single-particle Schrödinger equation embedded in the continuum of positive energy states. Their analysis was examined by Stillinger and Herrick [2] in the context of possible bound states (BICs) in atoms and molecules. It was demonstrated by Newton [3] that strong coupling between scattering channels can give rise to bound states in continuum. Bound states in continuum can be observed in the stationary transmission as resonant states with a width that tends to zero as at least two physical parameters vary continuously as was formulated by Friedrich and Wintgen [4], who also gave the example of a hydrogen atom in a magnetic field. Such a BIC is a very fragile structure. A small perturbation transforms it into narrow resonance. Nevertheless, Capasso et al. [5] reported direct evidence for BICs in a semiconductor superlattice.

For better understanding of the phenomenon of BICs in transport through electronic devices, it is useful to study as simple a quantum system as possible. Robnik [6] showed that a simple separable two-dimensional Hamiltonian can develop BIC under perturbation of open channels. An explicit proof of the existence of BICs was presented recently by Cederbaum et al. [7] in a molecular system if the electronic and the nuclear motions are coupled. In the present letter, we consider open Aharonov–Bohm (AB) rings, which are good candidates to observe BICs for an external magnetic field, and the energy of the incident electron can be easily varied experimentally. Moreover, the one-dimensional AB rings allow one to treat BICs wholly analytically. A phenomenon of zero resonance widths at discrete val-

ues of the energy of an incident particle and some relevant physical parameter was established in many works [8–16] since the work by Shahbazyan and Raikh, among them external magnetic flux was considered in [17, 18]. In this letter, we focus on the scattering wave function in the vicinity of and at a BICs point and how BIC participates in transport.

2. ONE-DIMENSIONAL RING

Following Xia [19], we write the wave functions in the segments of the structure shown in the inset of Fig. 1 as
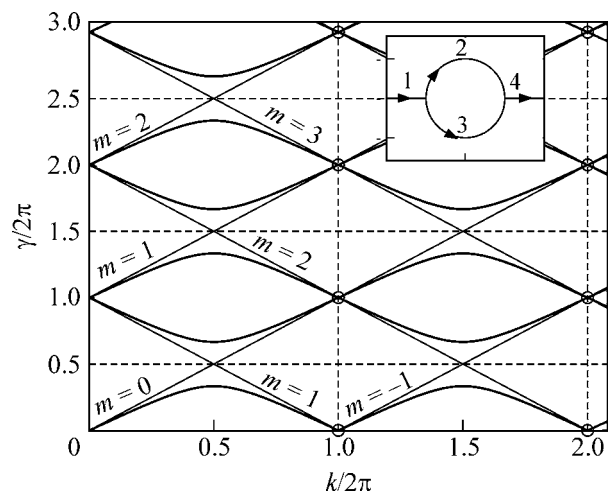

Fig. 1. Transmission zeros $|t|^2 = 0$ and ones $|t|^2 = 1$ of the one-dimensional ring as a function of the wave number k and flux γ. The zeros (ones) are shown by dashed (solid) lines. The thin solid lines represent the eigenenergies of the closed ring.

$$\psi_1(x) = \exp(ikx) + r\exp(-ikx),$$

$$\psi_2(x) = a_1\exp(ik^-x) + a_2\exp(-ik^+x),$$

$$\psi_3(x) = b_1\exp(ik^+x) + b_2\exp(-ik^-x),$$

$$\psi_4(x) = t\exp(ikx),$$

(1)

where $k^- = k - \gamma$, $k^+ = k + \gamma$, $\gamma = 2\pi\Phi/\Phi_0$, $\Phi = B\pi R^2$ is the magnetic flux and $\Phi_0 = 2\pi\hbar c/e$. The ring length $2\pi R$ is chosen as a unit. The boundary conditions (the continuity of the wave functions and the conservation of the current density) allow one to find all the coefficients in (1). We write the corresponding equation in the matrix form

$$\hat{F}\psi = g,$$

(2)

where $\hat{F}(k, \gamma)$ is the following matrix

$$
\begin{pmatrix}
-1 & 0 & 1 & 1 & 0 & 0 \\
-1 & 0 & 0 & 0 & 1 & 1 \\
0 & -1 & e^{ik^-/2} & e^{-ik^+/2} & 0 & 0 \\
0 & -1 & 0 & 0 & e^{ik^+/2} & e^{-ik^-/2} \\
1 & 0 & \dfrac{k^-}{k} & -\dfrac{k^+}{k} & \dfrac{k^+}{k} & -\dfrac{k^-}{k} \\
0 & -1 & \dfrac{k^-}{k}e^{i\frac{k^-}{2}} & -\dfrac{k^+}{k}e^{-i\frac{k^+}{2}} & \dfrac{k^+}{k}e^{i\frac{k^+}{2}} & -\dfrac{k^-}{k}e^{-i\frac{k^-}{2}}
\end{pmatrix},
$$

(3)

$g^T = (1\ 1\ 0\ 0\ 1\ 0)$. The vector $\psi^T = (r\ t\ a_1\ a_2\ b_1\ b_2)$ is the solution for the scattering wave function:

$$r = 2(3\cos k - 4\cos\gamma + 1)/Z,$$

$$t = 16i\left(\sin\frac{k}{2}\cos\frac{\gamma}{2}\right)/Z,$$

$$a_1 = 2(2e^{i\gamma} - 3e^{-ik} + 1)/Z,$$

$$a_2 = 2(e^{ik} + 1 - 2e^{i\gamma})/Z,$$

$$Z = 8\cos\gamma - 9e^{-ik} - e^{ik} + 2,$$

(4)

$b_{1,2}(k, \gamma) = a_{1,2}(k, -\gamma)$. In Fig. 1, we show lines of the transmission zeros ($|t(k, \gamma)| = 0$, dashed lines) that cross the lines of the transmission ones ($|t(k, \gamma)| = 1$, solid lines) at the points

$$k_m = 2\pi m, \quad m = \pm1, \pm2, \ldots,$$

$$\gamma_n = 2\pi n, \quad n = 0, \pm1, \pm2, \ldots.$$

(5)

As can be seen from the expression for the denominator Z in Eqs. (1), the imaginary part of the poles vanishes at these points. Simultaneously, at these points, there is a degeneracy of the eigenenergies of the closed ring ($k_m - \gamma)^2$. Here, m is the magnetic quantum number that defines the eigenfunctions of the closed ring $\psi_m(x) = $

$\exp(ik_m x)$. The point $k = 0$ is excluded from the consideration since it gives zero conductance. The particular points (5) were shown in [17] for the case of a single lead attached to the 1d ring. To show that BICs appear at points (5), let us consider one of the points, for example, $s_0 = (k_1, \gamma_1) = 2\pi(1, 1)$. All the other points are equivalent because of the periodic dependence of the system on k and γ. In the vicinity of the point s_0, we write Eqs. (1) in the following approximated form:

$$t \approx \frac{\Delta k}{\Delta k + i(\Delta\gamma)^2/2}, \quad r \approx \frac{i(3\Delta k^2 - 4\Delta\gamma^2)}{4(2\Delta k + i\Delta\gamma^2)},$$

$$a_1 \approx \frac{3\Delta k + 2\Delta\gamma}{4\Delta k + 2i\Delta\gamma^2}, \quad a_2 \approx \frac{\Delta k - 2\Delta\gamma}{4\Delta k + 2i\Delta\gamma^2},$$

(6)

where $\Delta k = k - k_1$, $\Delta\gamma = \gamma - \gamma_1$. The transmission amplitude in the vicinity of the point s_0 in (6) is similar to the expressions obtained for a shifted von Neumann–Wigner potential [20]. One can see that all the amplitudes $a_{1,2}$, $b_{1,2}$ of the inner wave functions are singular at the point s_0. Such a result for the BIC points was first found by Pursey and Weber [20].

Equations (2) and (3) allow one to show that the point s_0 corresponds to the BIC one in an open one-dimensional ring. At this point, matrix (3) takes the following form:

$$
\hat{F}(s_0) = \begin{pmatrix}
-1 & 0 & 1 & 1 & 0 & 0 \\
-1 & 0 & 0 & 0 & 1 & 1 \\
0 & -1 & 1 & 1 & 0 & 0 \\
0 & -1 & 0 & 0 & 1 & 1 \\
1 & 0 & 0 & -2 & 2 & 0 \\
0 & -1 & 0 & -2 & 2 & 0
\end{pmatrix}.
$$

(7)

The determinant of the matrix $\hat{F}(s_0)$ equals zero. Therefore, $\hat{F}f_0 = 0$. By direct substitution of the vector $f_0^T = \frac{1}{2}(0\ 0\ 1\ -1\ -1\ 1)$, one can verify that f_0 is the right eigenvector that is the null vector. The corresponding left null eigenvector is $\tilde{f}_0 = \frac{1}{2}(-1\ 1\ 1\ -1\ 0\ 0)$. It is well known from linear algebra that, if the determinant of matrix $\hat{F}$ is equaled to zero, then the necessary and sufficient condition for the existence of a solution of equation (2) is that the vector $\tilde{f}_0$ is orthogonal to the vector g [21]. It holds indeed that $\tilde{f}_0 \cdot \vec{g} = 0$. The solution of Eq. (2) at the point s_0 can therefore be presented as

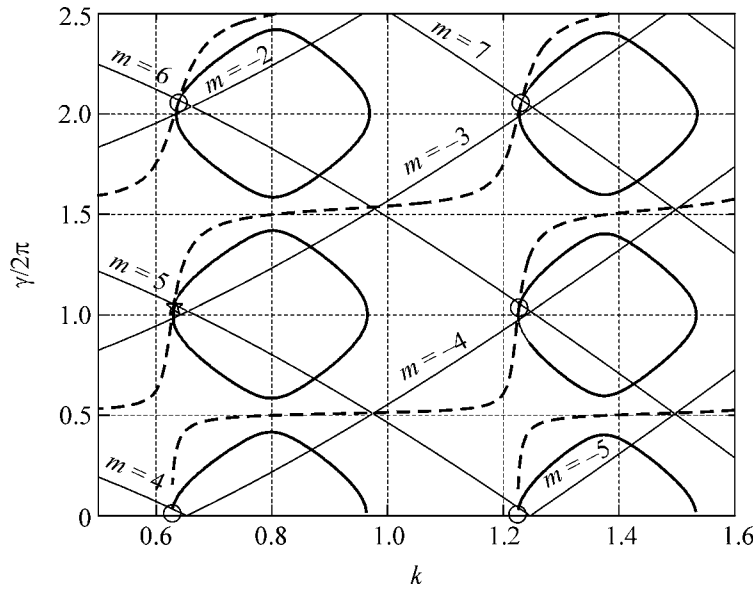$$\psi(s_0) = \alpha f_0 + \psi_p,$$

(8)

Fig. 2. Zeros (dashed lines) and ones (solid lines) of the transmission probability of the two-dimensional ring as a function of the wave number $k = \sqrt{E - \pi^2}$ and flux $\gamma = B\pi R^2 / \Phi_0$, $\Phi_0 = 2\pi\hbar c/e$. $R = 2.5$ is the mean radius of the ring. The width of the ring and those of the leads are equaled to a unit. The eigenenergies of the closed two-dimensional ring are shown by thin lines. The BIC points are marked by open circles and a star.

where α is an arbitrary coefficient and ψ_p is a particular transport solution of Eq. (2). By direct substitution, one can verify that $\psi_p^T = \begin{pmatrix} 0 & 1 & \frac{3}{4} & \frac{1}{4} & \frac{3}{4} & \frac{1}{4} \end{pmatrix}$ is the particular solution of Eq. (2). It is worthwhile to note that this result completely agrees with the scattering theory on graphs [22, 23]. Texier [22] has shown that, for certain graphs, the stationary scattering state gives the solution of the Schrödinger equation for the continuum spectrum apart for a discrete set of energies where some additional states are localized in the graph and thus are not probing by scattering, leading to the failure of the state counting method from the scattering.

In the vicinity of the BIC point s_0, the scattering state using (6) becomes, to the leading order of Δk, $\Delta \gamma$,

$$\psi(\mathbf{s}) \approx \frac{\Delta\gamma \mathbf{f}_0 + \Delta k \psi_p}{\Delta k + i\Delta\gamma^2/2}, \qquad (9)$$

where $\mathbf{s} = (k, \gamma)$. Thus, the scattering state in the nearest vicinity of the BIC point also is superposed of the BIC vector $\mathbf{f}_0$ and of the particular solution ψ_p. Equation (9) shows that the limiting scattering wave state ψ depends on the way $\mathbf{s} \longrightarrow \mathbf{s}_0$. If we at first take $\Delta\gamma = 0$, then we obtain $\psi = \psi_p$, which is a transport solution. If we, however, first choose $\Delta k = 0$, then we have $\psi = \frac{2}{i\Delta\gamma}\mathbf{f}_0$; i.e., the scattering state is diverging the ring interior. This formula shows that the BIC state $\mathbf{f}_0$ can be extracted from the scattering state by a special limit in (9).

3. TWO-DIMENSIONAL DEVICES

Typical open two-dimensional structures are dots or rings with attached leads. Numerically, the transmissions through them are solved by finite-difference equations that are equivalent to the tight-binding lattice model [24, 25]. The case of the quantum dots was considered in [16]. Here, we present the results of computations for the two-dimensional ring with symmetrically attached identical leads. In Fig. 2, we show the transmission zeros (dashed lines) and the transmission ones (solid lines) for the single-channel transmission.

In order to find the positions and widths of the resonance states, we explore the nonhermitian effective Hamiltonian, which can be obtained by projection of the whole system onto the Hilbert space of a closed system [25–27]. The effective Hamiltonian in the basis of the closed system's eigenvectors can be written as [24, 25]

$$\langle b | H_{\text{eff}} | b' \rangle = E_b \delta_{bb'} - \sum_p \sum_{C=L,R} V_{b,p}^C V_{b',p}^C e^{ik_p^C}. \qquad (10)$$

Here, E_b and $|b\rangle$ are the eigenvalues and the eigenfunctions of the closed system C enumerates the left and right leads, and p enumerates the open channels of the leads. A formula to calculate the matrix elements $V_{b,p}^C$ is given in [26, 25]. Because of the energy dependence of the effective Hamiltonian, the positions and widths

of the resonance states are defined by the following nonlinear fixed point equations [27]:

$$E_\lambda = \mathrm{Re}(z_\lambda(\gamma, E)), \quad 2\Gamma_\lambda = -\mathrm{Im}(z_\lambda(\gamma, E)). \quad (11)$$

Here, z_λ are the complex eigenvalues of the effective Hamiltonian (10) $H_{\mathrm{eff}}|\lambda) = z_\lambda|\lambda)$ with the right eigenstates $|\lambda)$. All the points at which $\Gamma_\lambda = 0$, i.e., the width of the resonant transmission vanishes, are marked in Fig. 2 by open circles and a star.

The equation for the scattering wave function mapping onto the ring interior $|\psi_R\rangle$ can be derived from the Lippmann–Schwinger equation [25–27] and takes the following form

$$(H_{\mathrm{eff}} - E)|\psi_R\rangle = V^L|E, L, p = 1\rangle. \quad (12)$$

Here, V^L is the coupling matrix between the left lead and the ring provided that a particle is incident from the left lead in the first channel. This formula is similar to (2) for the 1d ring. If $\mathrm{Det}(H_{\mathrm{eff}} - E) \neq 0$, then, in the biorthogonal basis $|\lambda)$, the scattering wave function takes a simple form [25, 27]

$$|\psi_R\rangle = \sum_\lambda \frac{V_\lambda(\gamma, E)}{E - z_\lambda(\gamma, E)}|\lambda), \quad (13)$$

where

$$V_\lambda = (\lambda|V|E, L, p = 1) = \int dy_B \tilde{\psi}_\lambda(y_B)\sin(\pi y_B), (14)$$

$\tilde{\psi}_\lambda$ are the left eigenfunctions of H_{eff}, and y_B runs over the boundary that connects the closed ring and the left lead with the first channel excited ($p = \mathrm{I}$). We assume that the magnetic field subjects only the ring.

Let us denote a set of physical parameters of the system as $\mathbf{s}$. For example, for the present case of the ring, $\mathbf{s} = (E, \gamma)$, although, for the quantum dot, $\mathbf{s}$ might be the energy and confined potential [16]. Let us consider the point $\mathbf{s}_0 = (E_0, \gamma_0)$ at which Eq. (11) is fulfilled: $E_0 = z_{\lambda_0}(E_0, \gamma_0)$ and $\Gamma_{\lambda_0} = 0$; i.e., one of the complex eigenvalues of H_{eff} is real at this point. For $E = E_0$, one has the equality $(H_{\mathrm{eff}} - E)|\lambda_0) = 0$. Comparing this equation to (12), we see that the eigenstate $|\lambda_0)$ corresponds to the solution of the Lippmann–Schwinger equation if there was no ingoing current in the left lead. Correspondingly, the state $|\lambda_0)$ cannot give rise to outgoing currents because of the continuity equation for the current density. In order to fulfill that, we have to consider that the eigenfunction ψ_{λ_0} does not overlap the first channel of the left lead; i.e., $V^L_{\lambda_0}(\mathbf{s}_0) = 0$. This may also be established by consideration of the transmission amplitude [25]:

$$t = -2\pi i \sum_\lambda \frac{\langle E, L|V^L|\lambda)(\lambda|V^R|E, R\rangle}{E - z_\lambda}. \quad (15)$$

Because of the symmetry of the system relative to the left and right leads $\left|V^L_{\lambda_0}\right| = \left|V^R_{\lambda_0}\right|$. In approaching the point $\mathbf{s} \longrightarrow \mathbf{s}_0$, the denominator $E - z_{\lambda_0}(\mathbf{s}) \longrightarrow 0$. Therefore, in order for the ratio $\left|V^L_{\lambda_0}(\mathbf{s})\right|^2/(E - z_{\lambda_0}(\mathbf{s}))$ to remain finite in (15), it is necessary that $\left|V^L_{\lambda_0}(\mathbf{s})\right| \longrightarrow 0$ for $\mathbf{s} \longrightarrow \mathbf{s}_0$. Thus, at the BIC point, we have orthogonality of the right-hand state ($V|E, L, p = 1\rangle$) in Eq. (12) to the left eigenstate ($\lambda_0|$. Then, in full correspondence with the consideration of the 1d ring (Eq. (8)), we have the following solution for the scattering state interior to the ring:

$$|\psi_R(\mathbf{s}_0)\rangle = \alpha|\lambda_0(\mathbf{s}_0)) + |\psi_p(\mathbf{s}_0)\rangle, \quad (16)$$

where the coefficient α is arbitrary. The right eigenfunction $\psi_{\lambda_0(\mathbf{s}_0)}$ of the effective Hamiltonian is squared integrable and, therefore, is the BIC function shown in Fig. 3a. Although the BIC function is disconnected from the first channel of the left lead, it couples with the next channels $p > 1$ of the leads that are evanescent modes. As a result, the BIC function has exponentially small tails in the leads as might be seen from Fig. 3a. Moreover, the coupling of the 2d ring with the evanescent modes gives rise to (as Fig. 2 shows) the BIC points being close to but different from the points at which two eigenfunctions of the closed 2d ring classified by the magnetic quantum numbers m have the same energy. The evanescent modes have imaginary wave numbers k_p that effectively change the Hamiltonian of the closed ring by the matrix

$$\sum_{p \neq 1} \sum_{C = L, R} V^C_{b, p} V^C_{b', p} e^{-|k_p|} \sim (d/R)^2$$

via Eq. (10). Therefore, only for the limiting case of the 1d ring ($d/R \longrightarrow 0$), the BIC state consists of a pair of eigenstates of a closed ring as seen from Fig. 1 as was confirmed by computations.

In the vicinity of $\mathbf{s}_0$, the value $E - z_{\lambda_0}(E, \gamma)$ is small. Then, we can split the summation over λ in (13) by two parts, $\lambda = \lambda_0$ and $\lambda \neq \lambda_0$, and, similar to as in (8), write the scattering state as

$$|\psi_R(\mathbf{s})\rangle = \alpha(\mathbf{s})|\lambda_0(\mathbf{s})) + |\psi_p(\mathbf{s})\rangle, \quad (17)$$

where

$$\alpha(\mathbf{s}) = \frac{V_{\lambda_0}(\mathbf{s})}{E - z_{\lambda_0}(\mathbf{s})}, \quad (18)$$

$|\psi_p\rangle$ is the contribution of all the other resonances.

As it is different from the 1d ring, we can study the behavior of singular coefficient (18) only numerically. Let us encircle the BIC point (k_0, γ_0) according to the relations $\Delta k = r\cos\phi$, $\Delta\gamma = r\sin\phi$ as shown in Fig. 4a, where $k_0 = \sqrt{E_0 - \pi^2}$, r is the radius of the encircling.
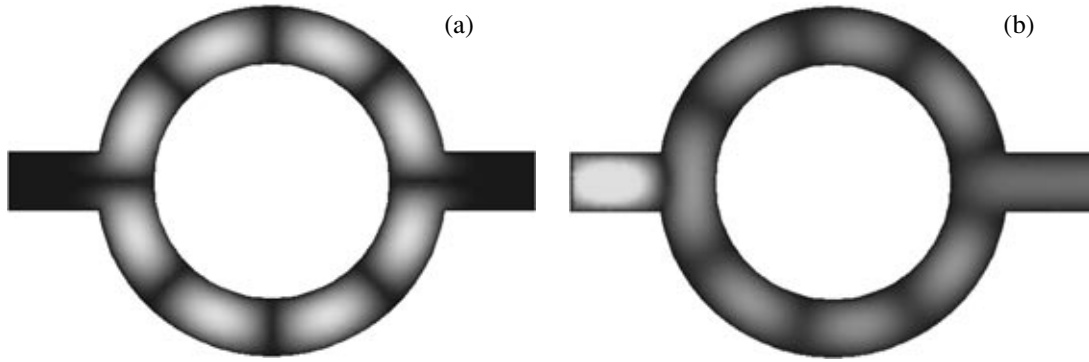
Fig. 3. The BIC function $\left|\psi_{\lambda_0}\right|$ that is the eigenfunction of the effective Hamiltonian (10) (a) and the transport solution $|\psi_p|$ (b) at the BIC point marked in Fig. 2 by a star.

Angular behaviors of quantities defining the parameter α are shown in Fig. 4b, 4c. In particular, the numeric shows that $|V_0(\mathbf{s})| \sim |\mathbf{s} - \mathbf{s}_0|^{1/2}$. The behavior of α in Fig. 4d is very similar to the behavior of the parameter $\alpha = \Delta\gamma/(\Delta k + i\Delta\gamma^2/2)$ for the 1d ring (see (9)) except that, in the 2d ring, we observe a phase difference. As one can see from Fig. 4d, at $\phi = 0$, π ($\Delta\gamma = 0$), the parameter $\alpha = 0$, and, at $\phi = \phi_0 < \pi/2$, $\alpha \longrightarrow \infty$. The angle ϕ_0 exactly corresponds to the direction of the tangential line of transmission zero shown by the dashed line in Fig. 2. Therefore, in order to extract the $|\psi_p\rangle$ from the scattering wave function (13), we should first put $\Delta\gamma = 0$ and then take the limit $\Delta k \longrightarrow 0$. If we take the limit to the BIC point along $\Delta\gamma = \tan(\phi_0)\Delta k$, the scattering state transforms to the BIC state $|\lambda_0\rangle$ shown in Fig. 3a. The particular solution for the scattering wave function $|\psi_p\rangle$ is shown in Fig. 3b.

Fig. 4. Angular behavior of quantities defining the parameter (18) around the BIC point marked by a star in Fig. 2.

4. CONCLUSIONS

Formulas (8) and (17) are the key ones that show that the scattering wave function ψ is not unique since the BIC can be superposed with the arbitrary coefficient α to ψ. Such a kind of decomposition was established recently for the scattering theory on graphs [22, 23]. Thus, at the point $\mathbf{s}_0$, the system becomes degenerate. The usual transport solution with energy $E = E_0$ is complemented by the squared integrable (localized interior to the ring) state $|\lambda_0(\mathbf{s}_0))$ with the same energy E_0 orthogonal to the former. The last state is, therefore, BIC. Our consideration shows exactly that BIC is the eigenvector of the nonhermitian effective Hamiltonian H_{eff} at the point at which the complex eigenvalue of H_{eff} becomes real and coincides with the energy of the incident particle. The scattering matrix is unique but not analytical at the BIC points as can be seen from formula (6). As seen from there, the transmission zeros cross the transmission ones at the BIC point. Note that these results are not restricted to only AB rings but are applicable for any open quantum system that allows varying at least two relevant physical parameters, for example, the energy of the incident particles and the shape of the billiard [16].

The bound state in continuum is disconnected from both single channel continua. In order to realize that the BIC is such a superposition of eigenstates of a closed system, overlapping (14) vanishes at BIC points. Specifically, in the present case of the AB ring attached to single channel leads, this superposition becomes an odd function relative to the even function of the leads as seen from Fig. 3a. For the 1d ring, nodes of the BIC are at points of connection of the ring to the leads, i.e., at those points, where the ratio of the lengths of the arms is rational [22]. However, for the 2d ring, the leads are attached exactly symmetrically, as shown in Fig. 3. It follows then that a violation of the symmetry of the system relative to the transport axis x leads to breakdown of the BIC. In particular, it occurs for a system disordered by impurities. In order for the BIC to survive under this violation of symmetry, one can use the
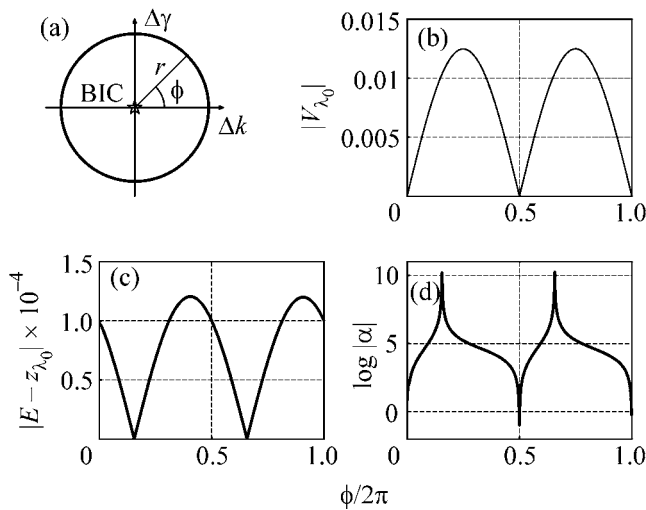
geometry given in [28] in which an infinite strip is attached to the ring. Moreover, the impurities lift a degeneracy of the closed ring [29]. However, as shown in [16], a condition for the BIC to survive is still remaining. From the above, it follows that, for the system symmetric about the y axis (the axis perpendicular to the transport axis), all the odd eigenstates of the closed system are BICs provided that the leads are excited in the first even channel. Then, a perturbation that lifts this symmetry transforms the BICs into resonance states whose widths are proportional to the perturbation. The external magnetic field that acts on only the ring is an example of such a perturbation.

The electron–electron interactions preserve the degeneracy of the closed ring [29]. They modify the energy spectrum and the coupling between the leads and the closed ring. As shown in [13], variation of the coupling changes the position of the BIC $\mathbf{s}_0$; however, it is not important to achieve a real value of the complex eigenvalue of the effective Hamiltonian. However, the Coulomb interactions might be important with respect to the fact that BICs can exhibit discrete charging similar to that predicted for resonance trapping in quantum dots strongly connected to the leads [30]. The strong coupling of a closed quantum system with leads ($\left| V_{b,\,p}^C \right| \gg |E_b - E_b|$ in terms of (10)) is hardly achievable while the existence of BICs is free of a value of the coupling between the closed system and continua.

Processes of inelastic scattering give rise to a finite resonance width. In that sense, BIC is a very subtle phenomenon for electron transmission. However, as formulas (9) and (17) show, the BIC state participates in the scattering wave function. If the above mentioned processes are efficiently small, the BIC state can dominate in the vicinity of the BIC point for a proper choice of the physical parameters, energy, and flux, as shown in Fig. 4d.

REFERENCES

1. J. von Neumann and E. Wigner, Phys. Z. **30**, 465 (1929).

2. F. H. Stillinger and D. R. Herrick, Phys. Rev. A **11**, 446 (1975).

3. R. G. Newton, *Scattering Theory of Waves and Particles*, 2nd ed. (Springer, Berlin, 1982; Mir, Moscow, 1969).

4. H. Friedrich and D. Wintgen, Phys. Rev. A **32**, 3231 (1985); Phys. Rev. A **32**, 3964 (1985).

5. F. Capasso, C. Sirtori, J. Faist, et al., Nature **358**, 565 (1992).

6. M. Robnik, J. Phys. A: Math. Gen. **19**, 3845 (1986).

7. L. S. Cederbaum, R. S. Friedman, V. M. Ryaboy, and N. Moiseyev, Phys. Rev. Lett. **90**, 13001 (2003).

8. T. V. Shahbazyan and M. E. Raikh, Phys. Rev. B **49**, 17 (1994); Phys. Rev. B **49**, 123 (1994).

9. O. Olendski and L. Mikhailovska, Phys. Rev. B **66**, 35331 (2002).

10. M. L. Ladron de Guevara, F. Claro, and P. A. Orellana, Phys. Rev. B **67**, 195335 (2003).

11. I. Rotter and A. F. Sadreev, Phys. Rev. E **69**, 66201 (2004); Phys. Rev. E **71**, 046204 (2005).

12. A. F. Sadreev, E. N. Bulgakov, and I. Rotter, JETP Lett. **82**, 498 (2005).

13. A. F. Sadreev, E. N. Bulgakov, and I. Rotter, J. Phys. A **38**, 10 647 (2005).

14. K. D. Rowe and P. J. Siemens, J. Phys. A: Math. Gen. **38**, 9821 (2005).

15. G. Ordonez, K. Na, and S. Kim, Phys. Rev. A **73**, 022113 (2006).

16. A. F. Sadreev, E. N. Bulgakov, and I. Rotter, Phys. Rev. B **73**, 235342 (2006).

17. B. Wunsch and A. Chudnovskiy, Phys. Rev. B **68**, 245317 (2003).

18. P. A. Orellana, M. L. Ladron de Guevara, and F. Claro, Phys. Rev. B **70**, 233315 (2004).

19. J.-B. Xia, Phys. Rev. B **45**, 3593 (1992).

20. D. L. Pursey and T. A. Weber, Phys. Rev. A **52**, 3932 (1995).

21. V. I. Smirnov, *A Course of Higher Mathematics*, 10th ed. (Nauka, Moscow, 1974; Pergamon, Oxford, 1964), Vol. 3, Part 1.

22. C. Texier, J. Phys. A: Math. Gen. **35**, 3389 (2002).

23. C. Texier and M. Büttiker, Phys. Rev. B **67**, 245410 (2003).

24. S. Datta, *Electronic Transport in Mesoscopic Systems* (Cambridge Univ. Press, Cambridge, 1995).

25. A. F. Sadreev and I. Rotter, J. Phys. A **36**, 11 413 (2003).

26. F. M. Dittes, Phys. Rep. **339**, 215 (2000).

27. J. Okołowicz, M. Płoszajczak, and I. Rotter, Phys. Rep. **374**, 271 (2003).

28. P. Exner, P. Seba, A. F. Sadreev, et al., Phys. Rev. Lett. **80**, 1710 (1998).

29. T. Chakraborty and P. Pietiläinen, Phys. Rev. B **50**, 8460 (1994); Phys. Rev. B **52**, 1932 (1995).

30. R. Berkovits, F. von Oppen, and J. W. Kantelhardt, Europhys. Lett. **68**, 699 (2004).